

Review

A Study of Chemical Processes of Nitrate in Atmospheric Aerosol and Snow Based on Stable Isotopes

Mengxue Chen ^{1,2}, Hewen Niu ^{1,2,*}  and Yankun Xiang ³

¹ State Key Laboratory of Cryospheric Sciences/National Field Science Observation and Research Station of Yulong Snow Mountain Cryosphere and Sustainable Development, Northwest Institute of Eco-Environment and Resources, Chinese Academy of Sciences, Lanzhou 730000, China; chenmengxue@nieer.ac.cn

² University of Chinese Academy of Sciences (UCAS), Beijing 100864, China

³ Nanjing Meteorological Bureau in Jiangsu Province, Nanjing 210019, China; xiangyankun233669@cma.cn

* Correspondence: niuhw@lzb.ac.cn

Abstract: Nitrate (NO_3^-) is a prominent atmospheric pollutant and a key chemical constituent of snow and ice, which plays a crucial role in the atmosphere and significantly impacts regional climate and environment conditions through a series of complex chemical processes. By summarizing the recent research progress on the nitrate chemical process (particularly on the isotopic measurements of NO_3^- ($\delta^{15}\text{N}$, $\Delta^{17}\text{O}$ and $\delta^{18}\text{O}$)) in atmosphere and glacier snow, this study mainly investigated the chemical compositions and chemical processes, formation pathways, and photochemical reactions of nitrate in snow and atmosphere. Our results identified that the main ways of atmospheric nitrate formation are the hydrolysis of N_2O_5 and the reaction of $\cdot\text{OH}$ with NO_2 ; the spatial distribution of $\Delta^{17}\text{O}$ and $\delta^{18}\text{O}$ values of atmospheric nitrate have a significant latitudinal trend between 30°N – 60°N ; the study of stable isotopes ($\delta^{15}\text{N}$ and $\delta^{18}\text{O}$) and the oxygen isotope anomaly ($\Delta^{17}\text{O}$) of nitrate have mainly been carried out over the densely populated and coastal mega cities; there exist significant gaps in the study of chemistry processes of nitrate in snow and ice and the air–snow interfaces across glaciated regions. This study provides a basic reference for more robust observations and research of nitrate in glacier areas in the future.

Keywords: nitrate; isotope composition; oxygen isotope anomaly; snow; formation pathway



Citation: Chen, M.; Niu, H.; Xiang, Y. A Study of Chemical Processes of Nitrate in Atmospheric Aerosol and Snow Based on Stable Isotopes. *Atmosphere* **2024**, *15*, 59. <https://doi.org/10.3390/atmos15010059>

Academic Editor: Akinori Ito

Received: 27 October 2023

Revised: 27 December 2023

Accepted: 28 December 2023

Published: 31 December 2023



Copyright: © 2023 by the authors. Licensee MDPI, Basel, Switzerland. This article is an open access article distributed under the terms and conditions of the Creative Commons Attribution (CC BY) license (<https://creativecommons.org/licenses/by/4.0/>).

1. Introduction

Nitrates are widely present in the surface environment and are an essential mineral of terrestrial ecosystems. They play a crucial role in the nitrogen cycle of the Earth system [1–4]. As one of the important components of atmospheric deposition, nitrate (NO_3^-) has a profound impact on the environment and ecosystem. Nitrate ion in the atmosphere is a key component of fine particulate matter ($\text{PM}_{2.5}$), accounting for more than 20% of the total mass of $\text{PM}_{2.5}$. In addition, nitrates are one of the key factors in the formation of acid rain, which has adverse effects on water quality and ecosystems [5–8]. The precursor of nitrate, NO_x ($\text{NO}_x = \text{NO} + \text{NO}_2$), is an important component of atmospheric pollutants. In recent years, with the rapid social and economic development, the content of nitrogen oxides (NO_x) in the atmosphere emitted by motor vehicle exhaust, fossil fuel combustion, thermal power plants, etc., has significantly increased. NO_x not only exacerbates global atmospheric pollution but also gradually becomes a scientific focus of international atmosphere and environmental science community [9–11]. In the atmosphere, the majority of NO_x undergoes various transformations to form nitric acid (HNO_3), and this process has a significant impact on the pH of atmospheric rainfall. The NO_x has a strong relation with ozone (O_3) and hydroxyl radicals ($\cdot\text{OH}$) in the atmosphere [1,12–15]. Therefore, it is crucial to study the formation pathways and chemical processes of atmospheric nitrate to improve our understanding of nitrate chemistry and advance the field of atmospheric environment.

Nitrogen (N) and its cycling in nitrates in atmospheric environment and glacier snow play important roles in the natural nitrogen cycle of the Earth system, offering valuable insights into the impacts of human activities on the atmospheric environment and ecosystem.

The stable isotopes of nitrate and the oxygen isotope anomaly of nitrate are essential parameters and analysis channels in investigating atmospheric nitrate and their sources, formation pathways, and chemical processes [14,16]. The stable isotopes, including ^{18}O , ^{17}O , ^{16}O , ^{15}N , and ^{14}N (Table 1), can be measured within the NO_3^- anion. Given the relatively lower abundance of heavier isotopes, the utilization of δ values is widespread for expressing the relative isotopic ratios, which is defined by the formula $\delta(\text{‰}) = \left(\frac{R_{\text{sample}}}{R_{\text{standard}}} - 1\right) \times 1000$ (Table 1), and according to the Vienna Standard Mean Ocean Water (VSMOW) for $\delta^{17}\text{O}$ and $\delta^{18}\text{O}$, the reference is gaseous N_2 for $\delta^{15}\text{N}$ [17]. In various biological, physical, and chemical reactions, the phenomenon where isotopes of a specific element distributed in different substances in varying proportions is referred to as isotope fractionation. Isotope fractionation related to mass is called mass-dependent fractionation (MDF). In this phenomenon, there is a linear relationship between $\delta^{17}\text{O}$ and $\delta^{18}\text{O}$, which is expressed as $\delta^{17}\text{O} = 0.52 \times \delta^{18}\text{O}$ [18,19]. This phenomenon is widely observed and identified in oxygen and water bodies. However, this linear relationship does not exist in the formation process of O_3 , which is known as mass-independent fractionation (MIF) of isotope [20–24]. The degree of MIF is generally determined and expressed by employing the oxygen isotopic anomaly ($\Delta^{17}\text{O}$): $\Delta^{17}\text{O} = \delta^{17}\text{O} - 0.52 \times \delta^{18}\text{O}$ (Table 1).

Table 1. Stable isotopes and isotopic anomalies of nitrate ion.

Name	Notation	Formula	Parametric
Stable isotope	$\delta^{18}\text{O}$		$R = ^{18}\text{O}/^{16}\text{O}$
Stable isotope	$\delta^{17}\text{O}$	$\delta(\text{‰}) = \left(\frac{R_{\text{sample}}}{R_{\text{standard}}} - 1\right) \times 1000$	$R = ^{17}\text{O}/^{16}\text{O}$
Stable isotope	$\delta^{15}\text{N}$		$R = ^{15}\text{N}/^{14}\text{N}$
Oxygen anomaly of nitrate ion	$\Delta^{17}\text{O}$		$\Delta^{17}\text{O} = \delta^{17}\text{O} - 0.52 \times \delta^{18}\text{O}$

The current scientific understanding of atmospheric and snow/ice chemistry remains incomplete. A large number of relevant studies primarily rely on numerical isotopic fractionation model, chemistry box model, and chemical transport model. These models have investigated oxygen isotopic anomalies in the atmosphere, the photolysis of nitrate in Antarctic ice/snow, and the formation processes of nitrate [14,25,26]. In addition, many studies on the chemical processes and formation pathways of atmospheric nitrates have been conducted in coastal cities of North America [12,13,27–29], some mega cities in Europe [28,30], and over the eastern coastal region of Asia [8,31–33]. The investigation of chemical processes of nitrate in glacier regions has significant implications for understanding atmospheric nitrogen oxide levels in the past. However, studies on nitrate chemical processes in glacier snow/ice and its formation pathways at the air–snow interface have been primarily carried out in the Antarctic ice sheet and Greenland ice sheet, while little relevant studies have been performed over mountain glaciers, leaving large gaps in understanding well the nitrate chemical processes over the cryosphere area. This study provides a comprehensive review of atmospheric nitrate chemistry and snow chemistry. Additionally, we propose the current study limitation and highlight the future research needs of nitrate chemistry of snow/ice.

2. Measurement Methods for Stable Oxygen Isotope

Currently, there are several methods available for determining the N and O isotopes of nitrates, including ion-exchange- AgNO_3 method [34], pyrolysis method [35], azide method [36], and denitrification bacteria method [24,37].

The ion-exchange- AgNO_3 method: The nitrate (NO_3^-) samples were individually combusted in a furnace and subjected to a high-temperature pyrolysis to produce N_2 and CO . The separated gases were introduced into an isotope ratio mass spectrometer (IRMS) through a chromatographic column for the analysis of $\delta^{15}\text{N}$ [38]. The oxygen isotopes ($\delta^{17}\text{O}$ and $\delta^{18}\text{O}$) were determined using the pyrolysis method. After purifying the nitrate (NO_3^-) samples, they were converted into AgNO_3 solution through ion exchange column and Ag_2SO_4 . The dried AgNO_3 powder was then heated in a high-temperature quartz reaction tube ($550\text{ }^\circ\text{C}$) to generate O_2 , NO_2 , Ag , and trace amounts of N_2 and NO . The generated gases were directed into a liquid nitrogen trap for enrichment, purification, and separation. Finally, the obtained oxygen gas (O_2) was introduced into an IRMS for the testing of oxygen isotope ratios [35].

The azide method: The first step involves using cadmium metal to reduce the amount of NO_3^- converted to NO_2^- . The second step is to reduce the generated NO_2^- to N_2O with the assistance of sodium azide and a weak acid buffer environment. Subsequently, the N_2O gas is thermally decomposed into N_2 and O_2 through a high-temperature metal tube, and then, they enter an IRMS for the determination of N and O isotopes [36].

The denitrification bacteria method: This method involves the direct conversion of NO_3^- to N_2O by denitrifying bacteria. Firstly, the cultivation of denitrifying bacteria requires the preparation of culture medium, cultivation liquid, and rinsing solution. The freeze-dried powder of golden pseudomonas bacteria is activated, followed by sealed cultivation. Afterwards, well-grown individual colonies with a golden yellow appearance are isolated and cultivated separately. Then, the cultivated denitrifying bacterial solution undergoes a series of processes, such as centrifugation, fractionation, and nitrogen blowing to remove N_2O gas from the culture liquid. Finally, the sample is injected into sample vials containing the bacterial solution for reaction. The obtained gas samples are purified, concentrated, and separated, and subsequently, their $\delta^{15}\text{N}$, $\delta^{17}\text{O}$, and $\delta^{18}\text{O}$ values are determined using an IRMS [37,39].

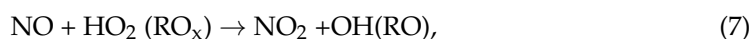
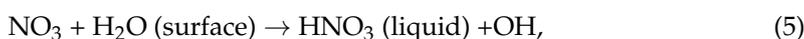
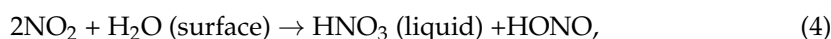
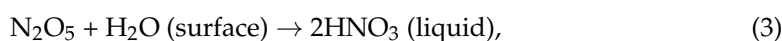
Among the four pre-treatment methods, the ion-exchange- AgNO_3 method and the azide method require a larger quantity of sample volume (with a higher detection limit) and involve a cumbersome process. Additionally, the azide method has a shorter pre-treatment time and higher accuracy, but it involves the use of highly toxic hazardous substances in the reaction. However, the denitrification bacteria method is simple to operate but has a low detection limit and can meet the required experimental accuracy. Thus, the denitrification bacteria method is one of the most widely applied methods for the detection of stable oxygen isotope of nitrate ion (NO_3^-).

3. Chemical Processes of Atmospheric Nitrate

On a global scale, the photolytic reactions of NO and $\cdot\text{OH}$, along with the hydrolysis of N_2O_5 , are commonly acknowledged as the dominant pathways for the formation of nitrates (Equations (1) and (2)) [26,40]. Chemical Equation (1)–(8) encompass the primary formation pathways of atmospheric nitrate (NO_3^-), whereas M in Equation (1) represents oxygen (O_2) and/or nitrogen (N_2) in the atmosphere, HC in Equation (3) represents hydrocarbons, and DMS stands for dimethyl sulfide. An improved GEOS-Chem simulation, incorporating $\Delta^{17}\text{O}$ of nitrate from various sites, revealed that both $\text{NO}_2 + \text{OH}$ (Equation (1)) and $\text{N}_2\text{O}_5 + \text{H}_2\text{O}$ (Equation (2)) contribute approximately 41% to global nitrate formation, and other mechanisms contribute less than 6% to near-surface nitrate levels globally [40]. The reaction between NO_2 and $\cdot\text{OH}$ primarily occurs during daylight hours. The reaction between NO_2 and O_3 generates N_2O_5 , which subsequently hydrolyzes to form HNO_3 , primarily taking place at night [26]. The contributions of different reactions vary greatly in different regions and periods. Due to the significant emissions of hydrocarbon compounds (HCS) in the atmosphere, the reaction between NO_3 and HC (Equation (3)) becomes an important pathway for the formation of industrial nitrates in industrial areas [41]. In non-coastal areas, the lower mixing ratio of DMS leads to a smaller contribution to the reaction of $\text{NO}_3 + \text{DMS}$ [42]. Studies have shown that in low temperature and heavily polluted

weather conditions, the absorption of N_2O_5 in aerosols and clouds is the primary pathway of nitrate formation [8,43]. Experiment-based research has indicated that the hydrolysis of NO_2 and NO_3 (Equations (4) and (5)) is not the main pathway for the formation of HNO_3 in the atmosphere due to their low reaction probabilities [44–46]. However, recent model simulations have reported that the hydrolysis of NO_2 (Equation (4)) is also an important source of HNO_3 formation in winter haze weather [47]. Additionally, it has been found that the heterogeneous reactions of NO_3 and N_2O_5 on the surface of aerosols are the main factors controlling the generation of nitrate in particulate matter during polluted weather conditions [48].

In general, there are two main oxidation pathways for NO to form NO_2 in the atmosphere. One is through the reaction of NO with O_3 (Equation (6)), and the other is through the oxidation of NO with OH/RO_2 (Equation (7)), followed by hydrolysis to form HNO_3 . HO_2/RO_2 represents peroxy radicals, which typically refer to a group of substances produced by reaction between certain organic groups (R) or hydrogen atoms with O_2 in the atmosphere [31]. NO_2 can also react with O_3 and generates NO_3^- radical (Equation (8)). The NO_3^- radical can react directly with hydrocarbons (HC) and dimethyl sulfide (DMS) and then generate HNO_3 , or it can undergo hydrolysis on the surfaces of aerosols to form HNO_3 [40,41]. The reaction of NO_3 with HC/DMS predominantly occurs during the night, because NO_3 is easily prone to photolysis during the daytime [49]. Nitrogen pentoxide (N_2O_5) is an active NO_x reservoir during the night, which can react at the surfaces of airborne particles, generating HNO_3 or both NO_2 and nitryl chloride (ClNO_2) (Equation (10)) [50]. Moreover, there are other potential mechanisms for the formation of nitrate particles, such as the hydrolysis of organic nitrates (RONO_2) and halogen nitrates (XNO_3), which play an important role in the formation of atmospheric nitrates in coastal areas and tropical rainforest [33]. Additionally, some halogens (X, such as Cl, Br, I) in polar regions can participate in photochemical reactions with NO_x , oxidizing and producing HNO_3 [51,52]. Taking bromine (Br) as an example, the halogen components typically undergo many reactions with nitric oxide and nitrate according to processes presented in Equations (11)–(14) to form nitric acid eventually [51].



Reactions indicated by Equations (7) and (12) represent the oxidation and photolysis of NO_x by O_3 , HO_2 , and RO_x after NO is emitted into the atmosphere. The cycle/transfer

between NO and NO₂ occurs quite rapidly, allowing them to establish a photochemical steady state during the day. The conversion of NO_x to nitrates is at least three orders of magnitude slower than the formation of NO and NO₂. The primary daytime reaction for the conversion of NO_x to nitrates involves the oxidation of NO₂ by ·OH to form HNO₃ (reaction 12, Equation (1)). Processes 5 to 11 in Figure 1 represent the formation pathways of nitrates during the nighttime. NO₂ reacts with O₃ (reaction 5, Equation (8)) to form NO₃, which then reacts with hydrocarbons (HC) to generate HNO₃ (reaction 8, Equation (3)). Alternatively, NO and NO₂ can inter-react to form N₂O₅ (reaction 7, Equation (9)), which undergoes heterogeneous reactions on the surfaces of aerosol to form HNO₃ (reaction 9, Equation (2)). Reactions 7 to 9 mainly occur at night since NO₃ is highly unstable during the day and rapidly undergoes photolysis, resulting in low concentrations [19,26].

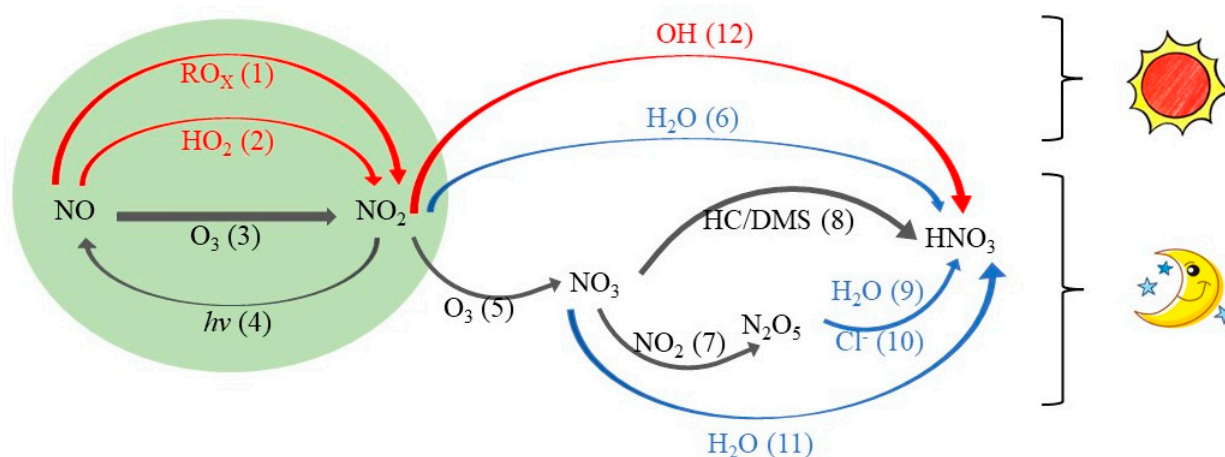


Figure 1. Schematic diagram illustrating main pathways of NO₃[−] formation in the atmosphere (reaction 1–reaction 12). Red font indicates reactions where the $\Delta^{17}\text{O}$ of the oxidants is close to zero, and blue font indicates processes of heterogeneous reactions in the atmosphere. (The figure was modified from [19].)

It is worth noting that heterogeneous reactions are also one of the main pathways to produce HNO₃. Simulations of atmospheric chemistry in the coastal areas of California using a chemistry box model have shown that over 50% of the nitrates in the summer atmosphere are generated from the reaction of NO₂ and ·OH, while over 90% of the nitrates in the winter atmosphere are produced through the heterogeneous reaction of N₂O₅ [14]. Nitrates in snow pits in Greenland are almost entirely generated from the reaction of NO₂ and ·OH in the summer, while in the winter, they are mainly produced through the reaction of NO₂ and O₃. Nitrates formed from the reaction of NO₃ and hydrocarbons account for about 40% of the total nitrate in the atmosphere, while the hydrolysis of N₂O₅ accounts for 60% of nitrate formation [19]. In addition, the reaction between N₂O₅ and Cl[−] is a heterogeneous reaction. Studies have shown that N₂O₅ reacts with Cl[−] released from coal-fired power plants to form ClNO₂ (reaction 10, Equation (9)), resulting in high concentrations of ClNO₂ in the atmosphere of North China [49,53,54]. Therefore, the reaction between N₂O₅ and Cl[−] is also noteworthy in severe polluted regions. Moreover, a higher relative humidity of atmosphere during nighttime than daytime creates favorable conditions for heterogeneous reactions, such as the hydrolysis of NO₃ (reaction 11, Equation (5)). These processes are crucial for the formation of nitrates during nighttime, with the pathways of (NO₃ + H₂O/HC) and (N₂O₅ + H₂O/Cl[−]) being the primary contributors. However, it should be emphasized that the heterogeneous reactions, especially the reaction (NO₂ + H₂O/OH), make comparable contributions to nitrate formation during both daytime and nighttime [31]. In wintertime, the low concentration of ·OH [55,56] and the high concentration of N₂O₅ in field measurements [57–59] highlight the significant contribution of N₂O₅ heterogeneous

reactions to nitrate formation in haze weather [60,61]. Additionally, during haze periods in North China, higher relative humidity and larger aerosol surface area facilitate the heterogeneous reactions of nitrogen oxides. Therefore, the reaction pathway of ($\text{NO}_2 + \text{H}_2\text{O}$) also serves as an important potential pathway for nitrate formation during haze events [55,62,63]. Moreover, it has been identified that the reactions among biogenic volatile organic compounds (BVOCs) and NO_x and NO_3 produce organic nitrates (e.g., RONO_2 , RO_2NO_2) [64]. Organic nitrate aerosols have the ability of absorbing sunlight, particularly in the ultraviolet (UV) range. Intense solar radiation and high temperature can lead to the increase of NO_x from nitrate photolysis, and a reduced source from organic nitrates can result in a short lifetime in the warmer air [40,65]. The formed RONO_2 undergoes oxidation reactions, yielding second-generation RONO_2 species. The photolysis and oxidation of those species can contribute to the recycling of NO_x [66]. Additionally, particle-phase RONO_2 ($p\text{RONO}_2$) contributes to the formation of organic aerosols. RONO_2 in the atmosphere is usually removed through dry/wet deposition or by subjecting it to hydrolysis to form inorganic nitrates and alcohols [67–69].

In polar regions, cold temperatures maintain/preserve the stability of HNO_4 formed from the reaction between HO_2 and NO_2 [70,71]. The presence of liquid HNO_4 enables further reactions with various chemical substances (such as HNO_2 , HSO_3^- , Cl^- , Br^- , and I^-) to form nitrates [51]. Therefore, heterogeneous chemical reactions play a crucial role in the formation of nitrates in polar regions. The specific reaction processes are illustrated by Equation (15)–(17), and Equation (17) specifically represents the reaction of halogens (X, such as Cl, Br, I) with HNO_4 [72–74].



4. Spatial Distribution of Isotopes of Atmospheric Nitrate

Nitrates is a significant form of nitrogen in the natural environment and can be readily utilized by organisms [75]. The values of $\delta^{15}\text{N}$, $\delta^{18}\text{O}$, and $\Delta^{17}\text{O}$ of nitrates have significant differences due to their different origins and sources. It has been demonstrated that the $\delta^{15}\text{N}(\text{NO}_x)$ in automobile exhaust is typically around -5% [76], while the $\delta^{15}\text{N}(\text{NO}_x)$ in atmospheric deposition ranges from -13% to 13% [77]. Synthetic fertilizers generally have $\delta^{15}\text{N}$ values ranging from -4% to 4% [78]. However, $\delta^{15}\text{N}$ alone cannot accurately indicate the different sources of nitrates. As such, the analysis of $\delta^{18}\text{O}$ and $\Delta^{17}\text{O}$ in nitrates becomes crucial in accurately identifying their sources. Integrating the data of $\delta^{15}\text{N}$, $\delta^{18}\text{O}$, and $\Delta^{17}\text{O}$ allows a more precise identification of the origins, formation conditions, and transfer pathways of nitrate formation.

Study of stable isotopes and isotopic anomalies of atmospheric nitrates is mainly focused on the coastal cities of Asia and North America and the western coast of Australia (Figure 2). However, there is a lack of investigation of atmospheric nitrates in glacier areas. High $\delta^{15}\text{N}$ values of atmospheric nitrate are distributed in the eastern coastal areas of Asia, the eastern coastal areas of North America, and the western coast of Australia. This is likely related to intensive anthropogenic emissions [76,77,79]. High $\Delta^{17}\text{O}$ values of atmospheric nitrate could also be found in the eastern coastal areas of Asia, the western coast of Australia, and the northern regions of North America, while high $\delta^{18}\text{O}$ values of atmospheric nitrate are spatially distributed along the western coast of Australia and the eastern United States. The different $\Delta^{17}\text{O}$ and $\delta^{18}\text{O}$ values of atmospheric nitrate are greatly influenced by atmospheric O_3 concentration and the pathways involved in its formation [12,24,80–83].

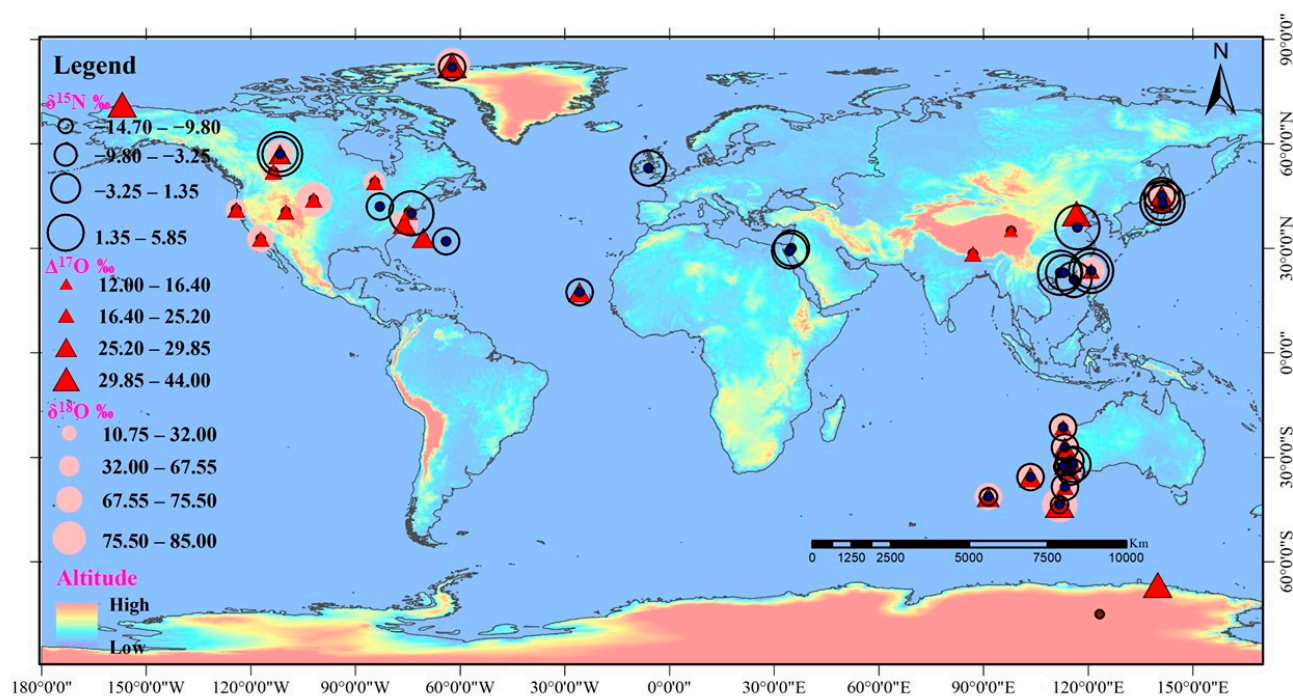


Figure 2. Spatial distribution of stable isotopes ($\delta^{15}\text{N}$, $\delta^{18}\text{O}$) and oxygen isotope anomaly ($\Delta^{17}\text{O}$) in atmospheric nitrate.

4.1. Investigation of $\delta^{15}\text{N}$ in Atmospheric NO_x

Formation of NO_3^- in the atmosphere primarily occurs through the oxidative reactions of NO_x . Atmospheric NO_x has both natural and anthropogenic sources. Natural sources include lightning, wildfires, microbial activities, and stratospheric transport. Anthropogenic sources primarily consist of the following: (1) fossil fuel combustion, such as emissions from coal-fired power plants and vehicle and aircraft exhaust emissions, (2) biomass burning emissions from agricultural waste (e.g., straw, sugarcane residue, rice husk) and household heating or cooking, and (3) agricultural activities, particularly fertilizer application, which significantly impacts the release of NO_x into the atmosphere [84]. Moreover, the dry and wet deposition of atmospheric NO_x is the main pathway/source of nitrate content in snow and ice. Stable nitrogen isotope of nitrate can be used to determine the origins and chemical processes of atmospheric nitrogen. The calculation method of nitrogen isotope ratios is as follows:

$$\delta^{15}\text{N}_{\text{sample}} (\text{‰}) = \left[\left(\frac{^{15}\text{N}}{^{14}\text{N}} \right)_{\text{sample}} / \left(\frac{^{15}\text{N}}{^{14}\text{N}} \right)_{\text{standard}} - 1 \right] \times 1000 \quad (18)$$

Different sources of NO_x have different $\delta^{15}\text{N}$ values, and emissions from fossil fuel combustion are the primary sources of NO_x in the atmosphere (e.g., automobile emission and coal combustion and power plant emissions) [79,85,86]. Stable nitrogen isotopes from natural sources (such as lightning and coal combustion) typically exhibit positive values [87–89]. Generally, NO_x from anthropogenic sources generated during the combustion process can be categorized into two types. The first is “thermal decomposition NO_x ,” which occurs at very high temperatures ($>2000\text{ }^\circ\text{C}$). Under high oxygen and pressure conditions in the combustion chamber, nitrogen and oxygen inter-reaction occurs, resulting in a typically negative $\delta^{15}\text{N}$ value. Examples of fuels that undergo thermal decomposition NO_x include diesel, gasoline, and natural gas. The second type is “combustion NO_x ,” which is formed during the combustion of nitrogen oxides in the fuel itself. As the reaction temperatures are not very high ($1300\text{--}1400\text{ }^\circ\text{C}$), the resulting $\delta^{15}\text{N}(\text{NO}_x)$ value is typically positive [90–92]. The $\delta^{15}\text{N}(\text{NO}_x)$ values contributed from the combustion of fossil fuels ranged from -17.9% to 19.8% (Figure 3) [79,85,86,93–95].

The $\delta^{15}\text{N}$ values of nitrogen-containing particles generated from fuel combustion are relatively small, mostly having negative values (-19.4‰ to 2.9‰) [95]. On the other hand, the $\delta^{15}\text{N}$ values of NO_x produced from coal combustion are relatively high (5.2‰ to 19.8‰) [79,86,93]. Different combustion conditions (temperatures of combustion, pressures, oxygen levels, biomasses, fossil fuels, etc.) of fossil fuels significantly influence nitrogen isotopes and their composition [86,95]. For example, diesel and gasoline have similar chemical properties, but their nitrogen isotope values are quite different (diesel: $+4.6\text{‰} \pm 0.8\text{‰}$; gasoline: $-7.5\text{‰} \pm 8.3\text{‰}$), which is due to their different combustion processes in terms of combustion temperature and oxygen content [95]. Moreover, the $\delta^{15}\text{N}$ values of NO_x in vehicle exhaust are lower (-13‰ to -2‰) compared to the values detected from power plant emitted exhausts (6‰ to 13‰). This is primarily due to the reaction ($\text{N}_2 + \text{O}_2 \leftrightarrow 2\text{NO}$) ($>2000\text{ °C}$) that favors the formation of lighter ^{14}N molecules, resulting in negative $\delta^{15}\text{N}(\text{NO}_x)$ values in vehicle exhaust [86]. In power plants, the reaction temperature is relatively low ($1300\text{--}1400\text{ °C}$), resulting in the low production of NO and a positive $\delta^{15}\text{N}(\text{NO}_x)$ value [86]. Notably, there exist significant differences in stable isotope values of nitrate from different sources. Factors contributing to these differences include combustion form, fuel type, chamber structure, and testing method. Therefore, it is necessary to conduct a detailed stable isotope analysis of nitrogen to better understand the exact sources, chemical processes, and formation pathways of nitrogen in atmosphere.

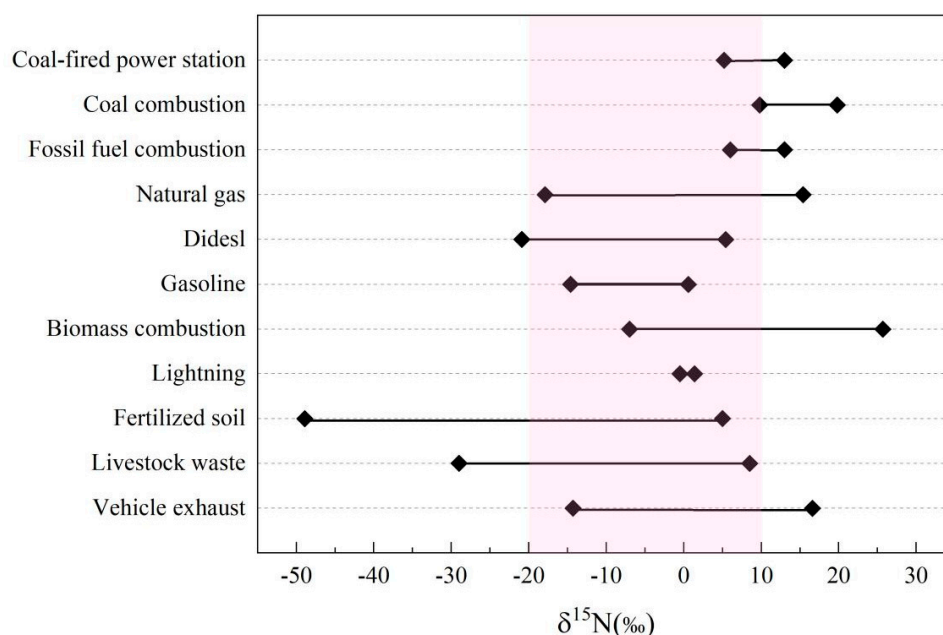


Figure 3. Distribution of $\delta^{15}\text{N}$ (‰) of atmospheric nitrate contributed from different sources.

4.2. Variability of $\delta^{18}\text{O}$ and $\Delta^{17}\text{O}$ of Atmospheric NO_3^-

The main oxidants that promote the conversion of NO_x to NO_3^- in the atmosphere are O_2 , O_3 , OH , HO_2/RO_2 , and XO . Figure 4 presents the spatial variations of $\delta^{18}\text{O}$ and $\Delta^{17}\text{O}$ of nitrates in the atmosphere across different latitudes at the global scale. There are two distinct patterns in both hemispheres. In the Northern Hemisphere, the $\delta^{18}\text{O}$ values of nitrate in the atmosphere significantly increase according to latitude gradients. The variation of $\delta^{18}\text{O}(\text{NO}_3^-)$ in the atmosphere is more obvious with notable fluctuations in low latitude regions ($30^\circ\text{ N--}60^\circ\text{ N}$). The variation of $\delta^{18}\text{O}(\text{NO}_3^-)$ with latitudes is primarily due to the gradient differences of oxygen isotope of O_3 in the atmosphere [80–82]. It is also caused by significant spatial differences in the formation pathways of NO_3^- [80,81]. The variation pattern of $\Delta^{17}\text{O}(\text{NO}_3^-)$ with latitude is similar to that of $\delta^{18}\text{O}(\text{NO}_3^-)$ in the atmosphere. The $\Delta^{17}\text{O}(\text{NO}_3^-)$ values in the atmosphere significantly increase along

high latitudes (60° N–80° N) in the Northern Hemisphere. The latitude variation of $\Delta^{17}\text{O}(\text{NO}_3^-)$ in the atmosphere is likely influenced by different formation pathways of nitrate [1,12,13,24,35,81].

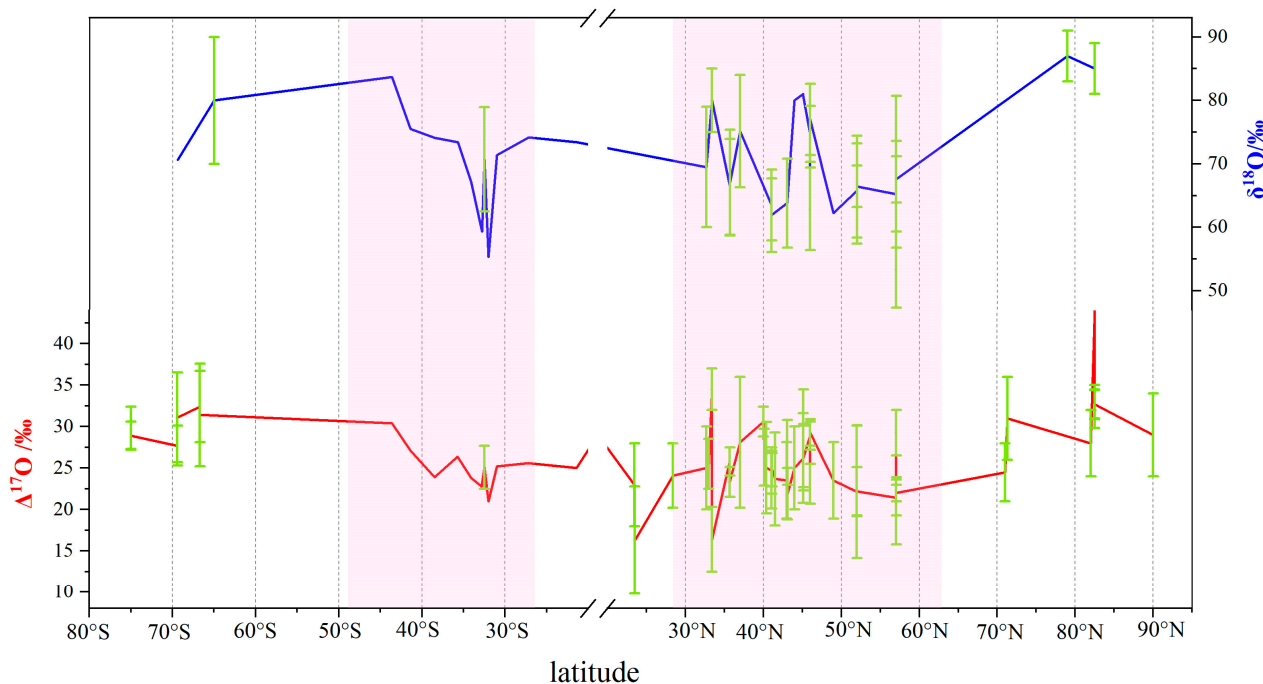


Figure 4. Latitude variations of $\Delta^{17}\text{O}(\text{NO}_3^-)$ and $\delta^{18}\text{O}(\text{NO}_3^-)$ in the atmosphere.

The characteristic values of $\Delta^{17}\text{O}(\text{NO}_3^-)$ and $\delta^{18}\text{O}(\text{NO}_3^-)$ in the atmosphere are both positive, with $\Delta^{17}\text{O}$ values being smaller than $\delta^{18}\text{O}$ values (15–30‰) (Figure 4). $\Delta^{17}\text{O}(\text{NO}_3^-)$ and $\delta^{18}\text{O}(\text{NO}_3^-)$ in the atmosphere exhibit clear seasonal variations [96]. The $\Delta^{17}\text{O}(\text{NO}_3^-)$ and $\delta^{18}\text{O}(\text{NO}_3^-)$ values in summer/spring are lower than those in winter. The seasonal variations of ozone content in the atmosphere have significant impacts on the $\Delta^{17}\text{O}$ and $\delta^{18}\text{O}$ values [1,15,97]. The correlation between $\Delta^{17}\text{O}$ and $\delta^{18}\text{O}$ values mainly lies in their similar seasonal variations. However, the driving factors behind the seasonal variations of $\Delta^{17}\text{O}$ and $\delta^{18}\text{O}$ are different [97]. The seasonal variation of $\delta^{18}\text{O}(\text{NO}_3^-)$ in the atmosphere is primarily influenced by the different oxidation pathways of NO_3^- in winter and summer, and the seasonal variation of O_3 concentration and light intensity. The $\delta^{18}\text{O}$ value of the O_3 pathway is higher than that of the $\cdot\text{OH}$ pathway. In the summer months, there is strong solar radiation, leading to a high degree of decomposition of volatile organic compounds (VOCs). As a consequence, the O_3 production rate decreases, leading to a greater generation of NO_3^- through the $\cdot\text{OH}$ pathway in the summer atmosphere. Conversely, during the winter months, there is relatively weaker solar radiation and a lower degree of VOCs decomposition, and the O_3 production rate increases, causing a higher proportion of NO_3^- produced through the O_3 pathway in the winter atmosphere [12–14]. The seasonal variation of $\Delta^{17}\text{O}(\text{NO}_3^-)$ values is due to seasonal differences in the oxidation pathways of NO_x [15,19]. Due to the photolysis of N_2O_5 , NO_3^- is primarily generated through the $(\text{NO}_2 + \cdot\text{OH})$ pathway during the day, while at night, it is mainly produced through the hydrolysis of N_2O_5 or the reaction of NO_3^- radicals with HC/DMS. Notably, the $\Delta^{17}\text{O}$ values in the N_2O_5 hydrolysis or the reaction of NO_3^- radicals with HC/DMS to form NO_3^- are higher than those in the $\cdot\text{OH}$ pathway [14,31]. In summer, there is a stronger radiation intensity and a longer duration of sunlight compared to winter, which results in the significant photolysis of N_2O_5 and indirectly leads to higher concentrations of $\cdot\text{OH}$. Consequently, lower $\Delta^{17}\text{O}$ values are observed in summer, while higher $\Delta^{17}\text{O}$ values are observed in winter. In addition, the seasonal variation of atmospheric water vapor content can impact the oxidation formation of NO_3^- . Higher water vapor content can facilitate the

generation of NO_3^- through the hydrolysis pathway of N_2O_5 , thus influencing the value of $\Delta^{17}\text{O}$ [32]. Currently, our understanding of the reaction processes involving NO_3^- in the atmosphere is still limited. The relative contributions of each process may vary; thus, more in-depth research employing chemical models is necessary to investigate the underlying mechanisms of the seasonal variations in $\Delta^{17}\text{O}(\text{NO}_3^-)$ and $\delta^{18}\text{O}(\text{NO}_3^-)$.

The generation process of nitrate ion (NO_3^-) in the atmosphere is rather complex. It is difficult to accurately determine the chemical pathways of nitrate solely through measuring $\Delta^{17}\text{O}$ of atmospheric nitrate. Currently, many studies combined measured $\Delta^{17}\text{O}(\text{NO}_3^-)$ with atmospheric chemistry models to further analyze the chemical pathways and formation mechanisms of atmospheric nitrate in various regions and seasons. Atmospheric chemistry models usually include chemistry box models, GEOS-Chem chemical transport models, and photochemical steady-state (PSS) [14,26,33,97]. For example, a chemistry box model has been employed to simulate the presence of nitrate in coastal aerosols in California, USA, and its simulation results were in good agreement with the experimental data during the spring and winter seasons [14]. However, a divergence emerged during the late summer and autumn, where the simulated values were found to be 2%–4% higher than the experimental measurements. This discrepancy can be attributed to the oversight of nitrate transport in the box model, highlighting the importance and necessity of considering the transport processes in precisely predicting atmospheric nitrate in coastal aerosols [14]. The results simulated from the chemistry box model indicate that during the spring season, the formation of nitrate primarily occurs through the hydrolysis of N_2O_5 and with high $\Delta^{17}\text{O}$ values, whereas during the summer, the higher oxidation of HO_2/RO_2 results in lower $\Delta^{17}\text{O}$ values. Simulations of $\Delta^{17}\text{O}$ values in the tropical marine boundary layer show that PSS more accurately stimulates $\Delta^{17}\text{O}$ variations, while GEOS-Chem still suffers from some errors due to the utilization of the photochemical steady-state equation at night [33,97].

5. Characteristics of Nitrogen–Oxygen Isotopes of Nitrates in Snow and Ice

Research on nitrates in snow and ice is primarily focused on the Antarctic region [25,81,98,99]. The concentration of NO_3^- in surface snow and ice in Antarctica ranges from 0.5 to 4.0 $\mu\text{eq L}^{-1}$. It increases gradually from coastal regions towards the interior of Antarctica. The NO_3^- concentration in snow and ice from Southwestern Antarctic is lower compared to that of the Southeastern Antarctic region. Emerging evidence from earlier research suggests an inverse correlation between NO_3^- concentration in Antarctic snow/ice and the rate of snow accumulation [100]. In addition, as the thickness of snow increases, NO_3^- concentration gradually decreases, which is attributed to wind drift and sastrugi formation in the vicinity of the sampling site [25]. The concentration changes of NO_3^- after deposition and isotopic fractionation is influenced by the evaporation of HNO_3 , the photolysis of NO_3^- , and the wind-driven redistribution of surface snow, causing a rapid decrease in the surface concentration of NO_3^- [101]. However, $\delta^{15}\text{N}(\text{NO}_3^-)$ values displayed an inverse trend with snow thickness and NO_3^- concentration. Strong enrichment of $\delta^{15}\text{N}(\text{NO}_3^-)$ in snow with increasing snow depth due to isotopic fractionation is caused by the mass loss of NO_3^- in the upper snowpack [102]. The variations of $\delta^{18}\text{O}$ and $\delta^{15}\text{N}$ along the vertical profiles of snow layer are opposite, as the snow depth increases, $\delta^{18}\text{O}$ values gradually decrease. The variation of $\Delta^{17}\text{O}$ along the depths of snow has a similar trend to that of $\delta^{18}\text{O}$, which is due to the fact that in NO_3^- deposition, the NO_3^- is formed secondarily after NO_3^- photolysis, and the isotopes of $\cdot\text{OH}$ and H_2O are exchanged, resulting in a decrease in $\delta^{18}\text{O}$ values, whereas the $\Delta^{17}\text{O}$ values of $\cdot\text{OH}$ and H_2O are close to zero, and the $\Delta^{17}\text{O}$ value decreases during the secondary NO_3^- formation [25,98]. This trend of NO_3^- and its isotopic composition usually can be observed in the low-accumulation regions of interior Antarctica and is mainly driven by the photolysis and recycling processes of NO_3^- [25,81,98,99,102]. Isotope analysis suggested that $\delta^{15}\text{N}(\text{NO}_3^-)$ in Antarctic snow ranges from -19.4% to 36.6% . The significant variation of $\delta^{15}\text{N}(\text{NO}_3^-)$ values likely indicates the fractionation

of nitrogen isotopes in the snow of Antarctica [81,103]. The NO_3^- and its $\delta^{15}\text{N}(\text{NO}_3^-)$ values exhibit similar spatial variation, namely, their values gradually increase from the coasts of East Antarctica towards/to the inland of Antarctica [81,99]. The $\delta^{18}\text{O}(\text{NO}_3^-)$ values in Antarctic snow and ice range from 12‰ to 101‰ (Table S1). The spatial variation of $\delta^{18}\text{O}(\text{NO}_3^-)$ is different compared with that of $\delta^{15}\text{N}$, and in areas with high snow accumulation rates along the Antarctic coast, the $\delta^{18}\text{O}(\text{NO}_3^-)$ values are higher, whereas in areas with lower accumulation rates in the inland, the $\delta^{18}\text{O}$ values are lower [99]. The spatial variation of $\delta^{18}\text{O}$ values of nitrate in Antarctic snow/ice is primarily influenced by the formation pathways of NO_3^- in snow layers. Additionally, once NO_x is deposited in snow layers, they will undergo consequent physical and chemical transformations. The products of NO_3^- photolysis undergo secondary oxidation reactions, leading to the regeneration of NO_3^- in surface snow and ice [103,104]. Moreover, it was reported that the $\Delta^{17}\text{O}(\text{NO}_3^-)$ values in Antarctic snow range from 13.2‰ to 44‰ [99,105]. The variation amplitude of $\Delta^{17}\text{O}(\text{NO}_3^-)$ is smaller compared to those of $\delta^{15}\text{N}$ and $\delta^{18}\text{O}$, suggesting that the spatial variation of $\Delta^{17}\text{O}(\text{NO}_3^-)$ in Antarctic snow is not obvious. The trend of $\Delta^{17}\text{O}(\text{NO}_3^-)$ is similar to that of $\delta^{18}\text{O}$, i.e., it gradually decreases from coastal areas to inland Antarctica [106].

6. Optical Properties of Nitrate in Snow and Ice

Higher concentrations of nitrate in snow and ice can lead to increased light absorption, affecting the albedo of surface snow/ice, which in turn can impact the energy exchange and flux between the Earth's surface and the atmosphere [25,107]. The deposition of NO_3^- from the atmosphere onto the surface of snow layers causes a series of complex physical and chemical reactions, which occur at the air-snow interface. During this process, in addition to NO_3^- concentration changes, the fractionation of nitrogen and oxygen isotopes in NO_3^- also takes place. The photochemical processes of NO_3^- in snow and ice can be described as follows, with reactions (19) and (20) being the main reactions of photolysis [108].



These photochemical reactions significantly affect NO_3^- concentrations in snow and play an important role in the transformation of nitrogen species and impact snow-pack chemistry [108,109]. The nitrogen and oxygen isotope fractionation coefficients (${}^{18}\epsilon = -34\%$ and ${}^{15}\epsilon = -48\%$) of NO_3^- photo-decomposition in Dome C ice core have been quantified [25,110]. Comparative results with the Rayleigh fractionation model indicate that ${}^{15}\epsilon$ has been underestimated. Snow samples exposed to ultraviolet radiation and placed in a closed laboratory environment greatly impact the photolysis and photo-decomposition of NO_3^- in snow. In this setting, the photolytic products such as NO_2 and OH were involved in subsequent NO_3^- generation and deposition, leading to the dilution of the isotopic ratios [102]. The secondary production of NO_3^- , as a result of the photolysis of NO_3^- , and the by-products (such as NO_2 and NO) of photolysis react with oxidants in the atmosphere, results in the variation of nitrogen isotopes [104,111]. Additionally, the photochemical decomposition of NO_3^- significantly affects the isotope changes in snow. Investigating and understanding the photochemical processes of NO_3^- in snow and ice is crucial for evaluating its environmental fate and impact on atmospheric composition.

7. Conclusions

The stable isotopes and isotopic anomalies of nitrate can be used to robustly trace the sources of NO_3^- and determine the oxidation pathways of NO_3^- and to understand the

chemical cycle of NO_3^- in multiple environmental media. This study mainly reviewed and synthesized the chemical processes of nitrate in atmosphere and snow/ice. The conclusions that can be drawn are as follows:

- (1) The formation of nocturnal atmospheric nitrates primarily occurs through the hydrolysis of N_2O_5 . During the daytime, the nitrates are mainly generated through the oxidation of NO_2 by OH radicals, resulting in the formation of HNO_3 . In summer, nitrates are mainly formed through the reaction of OH radicals with NO_2 , while in winter, the hydrolysis of N_2O_5 is the main process for the formation of atmospheric nitrate.
- (2) Research on stable isotopes and isotopic anomaly of atmospheric nitrate in glacier regions is scarce, especially in high-altitude glacier regions.
- (3) The $\Delta^{17}\text{O}$ and $\delta^{18}\text{O}$ values of nitrate in the atmosphere increase with latitude. The variation of $\delta^{18}\text{O}(\text{NO}_3^-)$ is more obvious with notable fluctuations in low-latitude regions (30°N – 60°N).
- (4) From the coastal areas to inland Antarctica, $\delta^{18}\text{O}(\text{NO}_3^-)$ values in snow and ice gradually decrease and $\delta^{15}\text{N}(\text{NO}_3^-)$ values increase. Photochemical reactions significantly facilitate the interaction of NO_x and NO_3^- at the air–snow interface, and greatly affect the NO_3^- concentration.

A study of the chemical processes of atmospheric nitrate and snow–ice nitrate in mountain glaciers is very rare and is currently in its initial stage. The study on the oxidation process of nitrate at the air–snow interface and in snow and ice of mountain glaciers has not been performed yet. Stable isotopes and isotopic anomaly of nitrate, as emerging techniques for the study of formation pathway and chemical processes of nitrate in atmosphere and snow/ice, can be used to examine/investigate the contribution of oxidation pathways of nitrate in high-altitude mountain glaciers. The study of nitrate isotopes in ice cores has not been conducted yet, which is an obvious research gap of cryosphere chemistry and can be bridged with the fields of climate study and environmental records. The study of chemical processes of nitrate in snow pits, ice cores, and the air–snow interface on glaciers needs a combination of numerical model simulation and extensive field observations of nitrate. Further study on the chemical processes of nitrate in the atmosphere and snow/ice is also needed to improve the understanding of its sources, formation mechanisms, and spatial–temporal variations.

Supplementary Materials: The following supporting information can be downloaded at: <https://www.mdpi.com/article/10.3390/atmos15010059/s1>, Table S1: Summary of values of $\Delta^{17}\text{O}(\text{NO}_x)$, $\delta^{18}\text{O}(\text{NO}_x)$, and $\delta^{15}\text{N}(\text{NO}_x)$ in Antarctic snow [81,99,112].

Author Contributions: Conceptualization, M.C.; methodology, Y.X.; software, Y.X.; formal analysis, M.C.; investigation, Y.X.; data curation, Y.X.; writing—original draft, M.C.; writing—review and editing, H.N.; visualization, H.N.; supervision, Y.X.; project administration, H.N.; funding acquisition, H.N.; validation, M.C.; Resources, H.N. All authors have read and agreed to the published version of the manuscript.

Funding: This research was funded by the National Natural Science Foundation of China, grant number: 41971080, and Youth Innovation Promotion Association CAS, grant number: 2021429.

Institutional Review Board Statement: Not applicable.

Informed Consent Statement: Not applicable.

Data Availability Statement: Not applicable.

Acknowledgments: This study was supported by the National Natural Science Foundation of China (41971080). We also thank the Youth Innovation Promotion Association CAS (2021429) for its support. We would also like to thank the experts for their support and help.

Conflicts of Interest: The authors declare no conflicts of interest.

References

1. Savarino, J.; Kaiser, J.; Morin, S.; Sigman, D.M.; Thiemens, M.H. Nitrogen and oxygen isotopic constraints on the origin of atmospheric nitrate in coastal Antarctica. *Atmos. Chem. Phys.* **2007**, *7*, 1925–1945. [[CrossRef](#)]
2. Gao, Z.M.; Zhang, F.Z. Research progress and perspectives on nitrogen cycle and pollution in the environment. *Environ. Sci. Ser.* **1982**, *4*, 7–12. (In Chinese)
3. Canfield, D.E.; Glazer, A.N.; Falkowski, P.G. The evolution and future of Earth's nitrogen cycle. *Science* **2010**, *330*, 192–196. [[CrossRef](#)] [[PubMed](#)]
4. Morin, S.; Savarino, J.; Frey, M.M.; Yan, N.; Bekki, S.; Bottenheim, J.W.; Martins, J.M.F. Tracing the Origin and Fate of NO_x in the Arctic Atmosphere Using Stable Isotopes in Nitrate. *Science* **2008**, *322*, 730–732. [[CrossRef](#)] [[PubMed](#)]
5. Wang, N.F.; Chen, Y.; Hao, Q.J.; Wang, H.B.; Yang, F.M.; Zhao, Q.; Bo, Y.; He, K.B.; Yao, Y.G. Seasonal variation and source analysis of the water-soluble inorganic ions in fine particulate matter in Suzhou. *Environ. Sci.* **2016**, *37*, 4482–4489. (In Chinese)
6. Fan, M.Y.; Cao, F.; Zhang, Y.Y.; Bao, M.Y.; Liu, X.Y.; Zhang, W.Q.; Gao, S.; Zhang, Y.L. Characteristics and source of water soluble inorganic ions in fine particulate matter during winter in Xuzhou. *Environ. Sci.* **2017**, *38*, 4478–4485. (In Chinese)
7. Huang, R.J.; Zhang, Y.; Bozzetti, C.; Ho, K.-F.; Cao, J.-J.; Han, Y.; Daellenbach, K.R.; Slowik, J.G.; Platt, S.M.; Canonaco, F.; et al. High secondary aerosol contribution to particulate pollution during haze events in China. *Nature* **2014**, *514*, 218–222. [[CrossRef](#)] [[PubMed](#)]
8. He, P.; Xie, Z.; Chi, X.; Yu, X.; Fan, S.; Kang, H.; Liu, C.; Zhan, H. Atmospheric $\Delta^{17}\text{O}$ (NO₃[−]) reveals nocturnal chemistry dominates nitrate production in Beijing haze. *Atmos. Chem. Phys.* **2018**, *18*, 14465–14476. (In Chinese) [[CrossRef](#)]
9. Zhang, W.Q.; Zhang, Y.L. Oxygen isotope anomaly ($\Delta^{17}\text{O}$) in atmospheric nitrate: A review. *Chin. Sci. Bull.* **2019**, *64*, 649–662. (In Chinese) [[CrossRef](#)]
10. Lamsal, L.N.; Martin, R.V.; Padmanabhan, A.; Zhang, Q.; Sioris, C.E.; Chance, K.; Kurosu, T.P.; Newchurch, M.J. Application of satellite observations for timely updates to global anthropogenic NO_x emission inventories. *Geophys. Res. Lett.* **2011**, *38*, 185–193. [[CrossRef](#)]
11. Kato, N.; Akimoto, H. Anthropogenic emissions of SO₂ and NO_x in Asia: Emission inventories. *Atmos. Environ. Part A Gen. Top.* **1992**, *26*, 2997–3017. [[CrossRef](#)]
12. Savard, M.M.; Cole, A.; Vet, R.; Smirnoff, A. The $\Delta^{17}\text{O}$ and $\delta^{18}\text{O}$ values of simultaneously collected atmospheric nitrates from anthropogenic sources—Implications for polluted air masses. *Atmos. Chem. Phys.* **2018**, *18*, 10373–10389. [[CrossRef](#)]
13. Morin, S.; Savarino, J.; Bekki, S.; Gong, S.; Bottenheim, J.W. Signature of Arctic surface ozone depletion events in the isotope anomaly ($\Delta^{17}\text{O}$) of atmospheric nitrate. *Atmos. Chem. Phys.* **2007**, *7*, 1451–1469. [[CrossRef](#)]
14. Michalski, G.; Scott, Z.; Kabling, M.; Thiemens, M.H. First measurements and modeling of $\Delta^{17}\text{O}$ in atmospheric nitrate. *Geophys. Res. Lett.* **2003**, *30*, GL017015. [[CrossRef](#)]
15. Morin, S.; Savarino, J.; Frey, M.M.; Domine, F.; Jacobi, H.W.; Kaleschke, L.; Martins, J.M.F. Comprehensive isotopic composition of atmospheric nitrate in the Atlantic Ocean boundary layer from 65° S to 79° N. *J. Geophys. Res. Atmos.* **2009**, *114*, D05303. [[CrossRef](#)]
16. Hoefs, J. *Stable Isotope Geochemistry*; Springer: Berlin/Heidelberg, Germany, 1973.
17. Criss, R.E. *Principles of Stable Isotope Distribution*; Oxford University Press: New York, NY, USA, 1999.
18. Matsuhisa, Y.; Goldsmith, J.R.; Clayton, R.N. Mechanisms of hydrothermal crystallization of quartz at 250-degrees-C and 15 Kbar. *Geochim. Cosmochim. Acta* **1978**, *42*, 173. [[CrossRef](#)]
19. Kunasek, S.A.; Alexander, B.; Steig, E.J.; Hastings, M.G.; Gleason, D.J.; Jarvis, J.C. Measurements and modeling of $\Delta^{17}\text{O}$ of nitrate in snowpits from Summit, Greenland. *J. Geophys. Res.* **2008**, *113*, JD010103. [[CrossRef](#)]
20. Miller, M.F. Isotopic fractionation and the quantification of ^{17}O anomalies in the oxygen three-isotope system: An appraisal and geochemical significance. *Geochim. Cosmochim. Acta* **2002**, *66*, 1881–1889. [[CrossRef](#)]
21. Meijer, H.A.J.; Li, W.J. The use of electrolysis for accurate $\Delta^{17}\text{O}$ and $\delta^{18}\text{O}$ isotope measurements in water. *Isot. Environ. Health Stud.* **1998**, *34*, 349–369. [[CrossRef](#)]
22. Luz, B.; Barkan, E. The isotopic ratios $^{17}\text{O}/^{16}\text{O}$ and $^{18}\text{O}/^{16}\text{O}$ in molecular oxygen and their significance in biogeochemistry. *Geochim. Cosmochim. Acta* **2005**, *69*, 1099–1110. [[CrossRef](#)]
23. Farquhar, J.; Savarino, J.; Jackson, T.L.; Thiemens, M.H. Evidence of atmospheric sulphur in the Martian regolith from sulphur isotopes in meteorites. *Nature* **2000**, *404*, 50–52. [[CrossRef](#)]
24. Kaiser, J.; Hastings, M.G.; Houlton, B.Z.; Röckmann, T.; Sigman, D.M. Triple oxygen isotope analysis of nitrate using the denitrifier method and thermal decomposition of N₂O. *Anal. Chem.* **2007**, *79*, 599–607. [[CrossRef](#)] [[PubMed](#)]
25. Frey, M.M.; Savarino, J.; Morin, S.; Erbland, J.; Martins, J.M.F. Photolysis imprint in the nitrate stable isotope signal in snow and atmosphere of East Antarctica and implications for reactive nitrogen cycling. *Atmos. Chem. Phys.* **2009**, *9*, 8681–8696. [[CrossRef](#)]
26. Alexander, B. Quantifying atmospheric nitrate formation pathways based on a global model of the oxygen isotopic composition ($\Delta^{17}\text{O}$) of atmospheric nitrate. *Atmos. Chem. Phys.* **2009**, *9*, 5043–5056. [[CrossRef](#)]
27. Patris, N.; Cliff, S.S.; Quinn, P.K.; Kasem, M.; Thiemens, M.H. Isotopic analysis of aerosol sulfate and nitrate during ITCT-2k2: Determination of different formation pathways as a function of particle size. *J. Geophys. Res. Atmos.* **2007**, *112*, D23301. [[CrossRef](#)]
28. Savarino, J.; Morin, S.; Erbland, J.; Grannec, F.; Patey, M.D.; Vicars, W.; Alexander, B.; Achterberg, E.P. Isotopic composition of atmospheric nitrate in a tropical marine boundary layer. *Proc. Natl. Acad. Sci. USA* **2013**, *110*, 17668–17673. [[CrossRef](#)] [[PubMed](#)]

29. Vicars, W.C.; Morin, S.; Savarino, J.; Wagner, N.L.; Erbland, J.; Vince, E.; Martins, J.M.F.; Lerner, B.M.; Quinn, P.K.; Coffman, D.J.; et al. Spatial and diurnal variability in reactive nitrogen oxide chemistry as reflected in the isotopic composition of atmospheric nitrate: Results from the CalNex 2010 field study. *J. Geophys. Res. Atmos.* **2013**, *118*, 10567–10588. [[CrossRef](#)]
30. Bourgeois, I.; Savarino, J.; Caillon, N.; Angot, H.; Barbero, A.; Delbart, F.; Voisin, D.; Clement, J.C. Tracing the fate of atmospheric nitrate in a subalpine watershed using $\Delta^{17}\text{O}$. *Environ. Sci. Technol.* **2018**, *52*, 5561–5570. [[CrossRef](#)]
31. Zhang, Y.L.; Zhang, W.; Fan, M.Y.; Li, J.; Fang, H.; Cao, F.; Lin, Y.C.; Wilkins, B.P.; Liu, X.; Bao, M.; et al. A diurnal story of $\Delta^{17}\text{O}(\text{NO}_3^-)$ in urban Nanjing and its implication for nitrate aerosol formation. *npj Clim. Atmos. Sci.* **2022**, *5*, 50. [[CrossRef](#)]
32. Qin, R.; Shi, G.T.; Chen, Z.L. Review of the study on the stable isotopes of nitrogen and oxygen in atmospheric nitrate. *Adv. Earth Sci.* **2019**, *34*, 124–139. (In Chinese) [[CrossRef](#)]
33. Nelson, D.M.; Tsunogai, U.; Ding, D.; Ohyama, T.; Komatsu, D.D.; Nakagawa, F.; Noguchi, I.; Yamaguchi, T. Triple oxygen isotopes indicate urbanization affects sources of nitrate in wet and dry atmospheric deposition. *Atmos. Chem. Phys.* **2018**, *18*, 6381–6392. [[CrossRef](#)]
34. Chang, C.; Langston, J.; Riggs, M.; Campbell, D.H.; Silva, S.R.; Kendall, C. A method for nitrate collection for delta $\delta^{15}\text{N}$ and $\delta^{18}\text{O}$ analysis from waters with low nitrate concentrations. *Can. J. Fish. Aquat. Sci.* **1999**, *56*, 1856–1864. [[CrossRef](#)]
35. Michalski, G.; Savarino, J.; Böhlke, J.K.; Thiemens, M. Determination of the total oxygen isotopic composition of nitrate and the calibration of a $\Delta^{17}\text{O}$ nitrate reference material. *Anal. Chem.* **2002**, *74*, 4989–4993. [[CrossRef](#)] [[PubMed](#)]
36. McIlvin, M.R.; Altabet, M.A. Chemical conversion of nitrate and nitrite to nitrous oxide for nitrogen and oxygen isotopic analysis in freshwater and seawater. *Anal. Chem.* **2005**, *77*, 5589–5595. [[CrossRef](#)] [[PubMed](#)]
37. Sigman, D.M.; Casciotti, K.L.; Andreani, M.; Barford, C.; Galanter, M.; Böhlke, J.K. A Bacterial Method for the Nitrogen Isotopic Analysis of Nitrate in Seawater and Freshwater. *Anal. Chem.* **2001**, *73*, 4145–4153. [[CrossRef](#)]
38. Soto, D.X.; Koehler, G.; Hobson, K.A. Combining Denitrifying Bacteria and Laser Spectroscopy for Isotopic Analyses ($\delta^{15}\text{N}$, $\delta^{18}\text{O}$) of Dissolved Nitrate. *Anal. Chem.* **2015**, *87*, 7000–7005. [[CrossRef](#)] [[PubMed](#)]
39. Casciotti, K.L.; Sigman, D.M.; Hastings, M.G.; Böhlke, J.K.; Hilkert, A. Measurement of the oxygen isotopic composition of nitrate in seawater and freshwater using the denitrifier method. *Anal. Chem.* **2002**, *4*, 4905–4912. [[CrossRef](#)]
40. Alexander, B. Global inorganic nitrate production mechanisms: Comparison of a global model with nitrate isotope observations. *Atmos. Chem. Phys.* **2020**, *20*, 3859–3877. [[CrossRef](#)]
41. Brown, S.S. Budgets for nocturnal VOC oxidation by nitrate radicals aloft during the 2006 Texas Air Quality Study. *J. Geophys. Res. Atmos.* **2011**, *116*, D24305. [[CrossRef](#)]
42. Preunkert, S.; Jourdain, B.; Legrand, M.; Udisti, R.; Becagli, S.; Cerri, O. Seasonality of sulfur species (dimethyl sulfide, sulfate, and methanesulfonate) in Antarctica: Inland versus coastal regions. *J. Geophys. Res. Atmos.* **2008**, *113*, D15302. [[CrossRef](#)]
43. Fan, M.-Y.; Zhang, Y.; Lin, Y.; Cao, F.; Zhao, Z.; Sun, Y.; Qiu, Y.; Fu, P.; Wang, Y. Changes of emission sources to nitrate aerosols in Beijing after the clean air actions: Evidence from dual isotope compositions. *J. Geophys. Res. Atmos.* **2020**, *125*, e2019JD031998. [[CrossRef](#)]
44. Burkholder, J.B.; Sander, S.P.; Abbatt, J.P.D.; Barker, J.R.; Huie, R.E.; Kolb, C.E.; Kurylo, M.J.; Orkin, V.L.; Wilmouth, D.M.; Wine, P.H. Chemical Kinetics and Photochemical Data for Use in Atmospheric Studies, Evaluation Number 18; California Institute of Technology: Pasadena, CA, USA, 2015).
45. Tan, F.; Tong, S.; Jing, B.; Hou, S.; Liu, Q.; Li, K.; Zhang, Y.; Ge, M. Heterogeneous reactions of NO_2 with $\text{CaCO}_3-(\text{NH}_4)_2\text{SO}_4$ mixtures at different relative humidities. *Atmos. Chem. Phys.* **2016**, *16*, 8081–8093. [[CrossRef](#)]
46. Crowley, J.N.; Ammann, M.; Cox, R.A.; Hynes, R.G.; Jenkin, M.E.; Mellouki, A.; Rossi, M.J.; Troe, J.; Wallington, T.J. Evaluated kinetic and photochemical data for atmospheric chemistry: Volume V—Heterogeneous reactions on solid substrates. *Atmos. Chem. Phys.* **2010**, *10*, 9059–9223. [[CrossRef](#)]
47. Chan, Y.; Evans, M.J.; He, P.; Holmes, C.D.; Jaeglé, L.; Kasibhatla, P.; Liu, X.; Sherwen, T.; Thornton, J.A.; Wang, X.; et al. Heterogeneous nitrate production mechanisms in intense haze events in the North China Plain. *J. Geophys. Res. Atmos.* **2021**, *126*, e2021JD034688. [[CrossRef](#)]
48. Wang, X.; Zhang, Y.; Chen, H.; Yang, X.; Chen, J.; Geng, F. Particulate nitrate formation in a highly polluted urban area: A case study by single-particle mass spectrometry in Shanghai. *Environ. Sci. Technol.* **2009**, *43*, 3061–3066. [[CrossRef](#)]
49. Wang, H.; Lu, K.; Guo, S.; Wu, Z.; Shang, D.; Tan, Z.; Wang, Y.; Le Breton, M.; Lou, S.; Tang, M.; et al. Efficient N_2O_5 uptake and NO_3 oxidation in the outflow of urban Beijing. *Atmos. Chem. Phys.* **2018**, *18*, 9705–9721. [[CrossRef](#)]
50. Thornton, J.A.; Kercher, J.P.; Riedel, T.P.; Wagner, N.L.; Cozic, J.; Holloway, J.S.; Dubé, W.P.; Wolfe, G.M.; Quinn, P.K.; Middlebrook, A.M.; et al. A large atomic chlorine source inferred from mid-continental reactive nitrogen chemistry. *Nature* **2010**, *464*, 271–274. [[CrossRef](#)]
51. Evans, M.J. Coupled evolution of BrO_x - ClO_x - HO_x - NO_x chemistry during bromine-catalyzed ozone depletion events in the Arctic boundary layer. *J. Geophys. Res.* **2003**, *108*, 8368. [[CrossRef](#)]
52. Saiz-Lopez, A.; Plane, J.M.C.; Mahajan, A.S.; Anderson, P.S.; Bauguitte, S.J.-B.; Jones, A.E.; Roscoe, H.K.; Salmon, R.A.; Bloss, W.J.; Lee, J.D.; et al. On the vertical distribution of boundary layer halogens over coastal Antarctica: Implications for O_3 , HO_x , NO_x and the Hg lifetime. *Atmos. Chem. Phys.* **2008**, *8*, 887–900. [[CrossRef](#)]
53. Zhou, W.; Zhao, J.; Ouyang, B.; Mehra, A.; Xu, W.; Wang, Y.; Bannan, T.J.; Worrall, S.D.; Priestley, M.; Bacak, A.; et al. Production of N_2O_5 and ClNO_2 in summer urban Beijing, China. *Atmos. Chem. Phys. Discuss.* **2018**, *349*, 11581–11597. [[CrossRef](#)]

54. Tham, Y.J.; Wang, Z.; Li, Q.; Yun, H.; Wang, W.; Wang, X.; Xue, L.; Lu, K.; Ma, N.; Bohn, B.; et al. Significant concentrations of nitryl chloride sustained in the morning investigations of the causes and impacts on ozone production in a polluted region of northern China. *Atmos. Chem. Phys.* **2016**, *16*, 14959–14977. [[CrossRef](#)]
55. Zheng, G.J.; Duan, F.K.; Su, H.; Ma, Y.L.; Cheng, Y.; Zheng, B.; Zhang, Q.; Huang, T.; Kimoto, T.; Chang, D.J.A.C.; et al. Exploring the severe winter haze in Beijing the impact of synoptic weather, regional transport and heterogeneous reactions. *Atmos. Chem. Phys.* **2015**, *15*, 2969–2983. [[CrossRef](#)]
56. Rao, Z.; Chen, Z.; Liang, H.; Huang, L.; Huang, D. Carbonyl compounds over urban Beijing Concentrations on haze and non-haze days and effects on radical chemistry. *Atmos. Environ.* **2016**, *124*, 207–216. [[CrossRef](#)]
57. Wang, H.; Chen, J.; Lu, K. Development of a portable cavity—Enhanced absorption spectrometer for the measurement ambient NO₃ and N₂O₅ experimental setup, lab characterizations, and field applications in a polluted urban environment. *Atmos. Meas. Tech.* **2017**, *10*, 1465. [[CrossRef](#)]
58. Wang, H.; Lu, K.; Chen, X.; Zhu, Q.; Chen, Q.; Guo, S.; Jiang, M.; Li, X.; Shang, D.; Tan, Z.; et al. High N₂O₅ concentrations observed in urban Beijing Implications of a large nitrate formation pathway. *Environ. Sci. Technol. Lett.* **2017**, *4*, 416–420. [[CrossRef](#)]
59. Li, Z.; Hu, R.; Xie, P.; Wang, H.; Lu, K.; Wang, D. Intercomparison of in situ CRDS and CEAS for measurements of atmospheric N₂O₅ in Beijing, China. *Sci. Total Environ.* **2018**, *613*, 131–139. [[CrossRef](#)]
60. Su, X.; Tie, X.; Li, G.; Cao, J.; Huang, R.; Feng, T.; Long, X.; Xu, R. Effect of hydrolysis of N₂O₅ on nitrate and ammonium formation in Beijing China WRF—Chem model simulation. *Sci. Total Environ.* **2017**, *579*, 221–229. [[CrossRef](#)]
61. Pathak, R.K.; Wu, W.S.; Wang, T. Summertime PM_{2.5} ionic species in four major cities of China nitrate formation in an ammonia deficient atmosphere. *Atmos. Chem. Phys.* **2009**, *9*, 1711–1722. [[CrossRef](#)]
62. Wang, J.; Zhang, X.; Guo, J.; Wang, Z.; Zhang, M. Observation of nitrous acid (HONO) in Beijing, China Seasonal variation, nocturnal formation and daytime budget. *Sci. Total Environ.* **2017**, *587*, 350–359. [[CrossRef](#)]
63. Tong, S.; Hou, S.; Zhang, Y.; Chu, B.; Liu, Y.; He, H.; Zhao, P.; Ge, M. Comparisons of measured nitrous acid (HONO) concentrations in a pollution period at urban and suburban Beijing, in autumn of 2014, in autumn of 2014. *Sci. China Chem.* **2015**, *58*, 1393–1402. [[CrossRef](#)]
64. Browne, E.C.; Cohen, R.C. Effects of biogenic nitrate chemistry on the NO_x lifetime in remote continental regions. *Atmos. Chem. Phys.* **2012**, *12*, 11917–11932. [[CrossRef](#)]
65. Kasibhatla, P.; Sherwen, T.; Evans, M.J.; Carpenter, L.J.; Reed, C.; Alexander, B.; Chen, Q.; Sulprizio, M.P.; Lee, J.D.; Read, K.A.; et al. Global impact of nitrate photolysis in sea-salt aerosol on NO_x, OH, and O₃ in the marine boundary layer. *Atmos. Chem. Phys.* **2018**, *18*, 11185–11203. [[CrossRef](#)]
66. Müller, J.F.; Peeters, J.; Stavrou, T. Fast photolysis of carbonyl nitrates from isoprene. *Atmos. Chem. Phys.* **2014**, *14*, 2497–2508. [[CrossRef](#)]
67. Xu, L.; Guo, H.; Boyd, C.M.; Klein, M.; Bougiatioti, A.; Cerully, K.M.; Hite, J.R.; Isaacman-VanWertz, G.; Kreisberg, N.M.; Knote, C.; et al. Effects of anthropogenic emissions on aerosol formation from isoprene and monoterpenes in the southeastern United States. *P. Natl. Acad. Sci. USA.* **2015**, *112*, 37–42. [[CrossRef](#)] [[PubMed](#)]
68. Rindelaub, J.D.; McAvey, K.M.; Shepson, P.B. The photochemical production of organic nitrates from α -pinene and loss via acid-dependent particle phase hydrolysis. *Atmos. Environ.* **2015**, *100*, 193–201. [[CrossRef](#)]
69. Jacobs, M.I.; Burke, W.J.; Elrod, M.J. Kinetics of the reactions of isoprene-derived hydroxynitrates: Gas phase epoxide formation and solution phase hydrolysis. *Atmos. Chem. Phys.* **2014**, *14*, 8933–8946. [[CrossRef](#)]
70. Legrand, M.; Preunkert, S.; Frey, M.; Bartels-Rausch, T.; Kukui, A.; King, M.D.; Savarino, J.; Kerbrat, M.; Jourdain, B. Large mixing ratios of atmospheric nitrous acid (HONO) at Concordia (east Antarctic plateau) in summer: A strong source from surface snow? *Atmos. Chem. Phys.* **2014**, *14*, 9963–9976. [[CrossRef](#)]
71. Dentener, F.; Williams, J.; Metzger, S. Aqueous phase reaction of HNO₄: The impact on tropospheric chemistry. *J. Geophys. Res. Atmos.* **2002**, *41*, 109–133.
72. Régimbal, J.M.; Mozurkewich, M. Peroxynitric acid decay mechanisms and kinetics at low PH. *J. Phys. Chem. A* **1997**, *101*, 8822–8829. [[CrossRef](#)]
73. Løgager, T.; Sehested, K. Formation and decay of peroxynitrous acid: A pulse radiolysis study. *J. Phys. Chem.* **1993**, *97*, 6664–6669. [[CrossRef](#)]
74. Amel, D.F. Trends in the structure of federally insured depository institutions. *Fed. Reserv. Bull.* **1996**, *82*, 1984–1994.
75. Mayer, B.; Boyer, E.W.; Goodale, C.; Jaworski, N.A.; van Breemen, N.; Howarth, R.W.; Seitzinger, S.; Billen, G.; Lajtha, K.; Nadelhoffer, K.; et al. Sources of nitrate in rivers draining sixteen watersheds in the northeastern U.S.: Isotopic constraints. *Biogeochemistry* **2002**, *57*, 171–197.
76. Miller, D.J.; Wojtal, P.K.; Clark, S.C.; Hastings, M.G. Vehicle NO_x emission plume isotopic signatures: Spatial variability across the eastern United States. *J. Geophys. Res. Atmos.* **2017**, *8*, 4698–4717. [[CrossRef](#)]
77. Kendall, C.; Elliott, E.M.; Wankel, S.D. Tracing Anthropogenic Inputs of Nitrogen to Ecosystems. In *Stable Isotopes in Ecology and Environmental Science*, 2nd ed.; Blackwell: Oxford, UK, 2007.
78. Wassenaar, L.I. Evaluation of the origin and fate of nitrate in the abbotsford aquifer using the isotopes of ¹⁵N and ¹⁸O in NO₃⁻. *Appl. Geochem.* **1995**, *10*, 391–405. [[CrossRef](#)]
79. Felix, J.D.; Elliott, E.M.; Shaw, S.L. Nitrogen isotopic composition of coal-fired power plant NO_x: Influence of emission controls and implications for global emission inventories. *Environ. Sci. Technol.* **2012**, *46*, 3528–3535. [[CrossRef](#)] [[PubMed](#)]

80. Freyer, H.D. Seasonal variation of $^{15}\text{N}/^{14}\text{N}$ ratios in atmospheric nitrate species. *Tellus Ser. B—Chem. Phys. Meteorol.* **1991**, *43*, 30–44. [[CrossRef](#)]
81. Shi, G.; Buffen, A.; Ma, H.; Hu, Z.; Sun, B.; Li, C.; Yu, J.; Ma, T.; An, C.; Jiang, S.; et al. Distinguishing summertime atmospheric production of nitrate across the East Antarctic Ice Sheet. *Geochim. Cosmochim. Acta.* **2018**, *231*, 1–14. [[CrossRef](#)]
82. Lyons, J.R. Transfer of mass-independent fractionation in ozone to other oxygen-containing radicals in the atmosphere. *Geophys. Res. Lett.* **2001**, *28*, 3231–3234. [[CrossRef](#)]
83. Vicars, W.C.; Savarino, J. Quantitative constraints on the ^{17}O -excess ($\Delta^{17}\text{O}$) signature of surface ozone: Ambient measurements from 50°N to 50°S using the nitrite-coated filter technique. *Geochim. Cosmochim. Acta* **2014**, *135*, 270–287. [[CrossRef](#)]
84. Li, D.J.; Wang, X.M. Nitrogen isotopic signature of soil-released nitric oxide (NO) after fertilizer application. *Atmos. Environ.* **2008**, *42*, 4747–4754. [[CrossRef](#)]
85. Felix, J.D.; Elliott, E.M. Isotopic composition of passively collected nitrogen dioxide emissions: Vehicle, soil and livestock source signatures. *Atmos. Environ.* **2014**, *92*, 359–366. [[CrossRef](#)]
86. Heaton, T.H.E. $^{15}\text{N}/^{14}\text{N}$ ratios of NO_x from vehicle engines and coal-fired power stations. *Tellus B* **1990**, *42*, 304–307. [[CrossRef](#)]
87. Hoering, T. The isotope composition of the ammonia and nitrate ion in rain. *Geochim. Et Cosmochim. Acta* **1958**, *12*, 97–102. [[CrossRef](#)]
88. Fibiger, D.L.; Hastings, M.G. First Measurements of the nitrogen isotopic composition of NO_x from biomass burning. *Environ. Sci. Technol.* **2016**, *50*, 11569–11574. [[CrossRef](#)] [[PubMed](#)]
89. Hastings, M.G. Evaluating source, chemistry and climate change based upon the isotopic composition of nitrate in ice cores. *IOP Conf. Ser. Earth Environ. Sci.* **2010**, *9*, 012002. [[CrossRef](#)]
90. Bowman, C.T. Kinetics of pollutant formation and destruction in combustion. *Prog. Energy Combust. Sci.* **1975**, *1*, 33–45. [[CrossRef](#)]
91. Hayhurst, A.N.; Vince, I.M. Nitric oxide formation from N_2 in flames: The importance of “prompt” NO. *Prog. Energy Combust. Sci.* **1980**, *6*, 35–51. [[CrossRef](#)]
92. Toof, J.L. A Model for the Prediction of Thermal, Prompt, and Fuel NO_x Emissions From Combustion Turbines. *J. Eng. Gas Turbines Power* **1986**, *108*, 340–347. [[CrossRef](#)]
93. Heaton, T.H.E. $^{15}\text{N}/^{14}\text{N}$ ratios of nitrate and ammonium in rain at Pretoria, South Africa. *Atmos. Environ.* **1987**, *21*, 843–852. [[CrossRef](#)]
94. Walters, W.W.; Tharp, B.D.; Fang, H.; Kozak, B.J.; Michalski, G. Nitrogen isotope composition of thermally produced NO_x from various fossil-fuel combustion sources. *Environ. Sci. Technol.* **2015**, *49*, 11363–11371. [[CrossRef](#)]
95. Widory, D. Nitrogen isotopes: Tracers of origin and processes affecting PM_{10} in the atmosphere of Paris. *Atmos. Environ.* **2007**, *41*, 2382–2390. [[CrossRef](#)]
96. Guha, T.; Lin, C.T.; Bhattacharya, S.K.; Mahajan, A.S.; Ou-Yang, C.F.; Lan, Y.P.; Hsu, S.C.; Liang, M.C. Isotopic ratios of nitrate in aerosol samples from Mt. Lulin, a high-altitude station in central Taiwan. *Atmos. Environ.* **2017**, *154*, 53–69. [[CrossRef](#)]
97. Morin, S.; Sander, R.; Savarino, J. Simulation of the diurnal variations of the oxygen isotope anomaly ($\Delta^{17}\text{O}$) of reactive atmospheric species. *Atmos. Chem. Phys.* **2011**, *11*, 3653. [[CrossRef](#)]
98. Berhanu, T.A.; Meusinger, C.; Erbland, J.; Jost, R.; Bhattacharya, S.K.; Johnson, M.S.; Savarino, J. Laboratory study of nitrate photolysis in Antarctic snow. II. Isotopic effects and wavelength dependence. *J. Chem. Phys.* **2014**, *140*, 244306. [[CrossRef](#)] [[PubMed](#)]
99. Erbland, J.; Vicars, W.C.; Savarino, J.; Morin, S.; Frey, M.M.; Frosini, D.; Vince, E.; Martins, J.M.F. Air-snow transfer of nitrate on the East Antarctic Plateau—Part 1: Isotopic evidence for a photolytically driven dynamic equilibrium in summer. *Atmos. Chem. Phys.* **2013**, *13*, 6403–6419. [[CrossRef](#)]
100. Arthern, R.J.; Winebrenner, D.P.; Vaughan, D.G. Antarctic snow accumulation mapped using polarization of 4.3 cm wavelength microwave emission. *Atmospheres* **2006**, *111*. [[CrossRef](#)]
101. Frey, M.M.; Stewart, R.W.; McConnell, J.R.; Bales, R.C. Atmospheric hydroperoxides in West Antarctica: Links to stratospheric ozone and atmospheric oxidation capacity. *J. Geophys. Res.* **2005**, *110*, D23301. [[CrossRef](#)]
102. Blunier, T.; Floch, G.L.; Jacobi, H.W.; Quansah, E. Isotopic view on nitrate loss in Antarctic surface snow. *Geophys. Res. Lett.* **2005**, *32*, L13501. [[CrossRef](#)]
103. Shi, G.T.; Qin, R.; Ma, H.M.; Hu, Z.Y.; An, C.L.; Jiang, S.; Li, Y.S. A Review of the stable isotopic composition of nitrate in Antarctic snow and ice east. *Chin. J. Polar Res.* **2019**, *31*, 117–127. (In Chinese)
104. McCabe, J.R.; Boxe, C.S.; Colussi, A.J.; Hoffman, M.R.; Thiemens, M.H. Oxygen isotopic fractionation in the photochemistry of nitrate in water and ice. *J. Geophys. Res.* **2005**, *110*, D15310. [[CrossRef](#)]
105. Buffen, A.; Hastings, M.G. The isotopic composition of nitrate in west Antarctica at present and since the last glacial stage. In Proceedings of the American Geophysical Union, Fall Meeting 2014, San Francisco C31C-0310 (2014), San Francisco, TX, USA, 15–19 December 2014.
106. Zatko, M.; Geng, L.; Alexander, B.; Sofen, E.; Klein, K. The impact of snow nitrate photolysis on boundary layer chemistry and the recycling and redistribution of reactive nitrogen across Antarctica and Greenland in a global chemical transport model. *Atmos. Chem. Phys.* **2016**, *16*, 2819–2842. [[CrossRef](#)]
107. Ginot, P.; Kull, C.; Schwikowski, M.; Schotterer, U.; Gäggeler, H.W. Effects of post depositional processes on snow composition of a subtropical glacier (Cerro Tapado, Chilean Andes). *J. Geophys. Res. Atmos.* **2001**, *106*, 32375–32386.

108. Mcfall, A.S.; Edwards, K.C.; Anastasio, C. Nitrate photochemistry at the air-ice interface and in other ice reservoirs. *Environ. Sci. Technol.* **2018**, *52*, 5710–5717. [[CrossRef](#)] [[PubMed](#)]
109. Dibb, J.E.; Arsenault, M.; Peterson, M.C.; Honrath, R.E. Fast nitrogen oxide photochemistry in Summit, Greenland snow. *Atmos. Environ.* **2002**, *36*, 2501–2511. [[CrossRef](#)]
110. Miller, C.E.; Yung, Y.L. Photo-induced isotopic fractionation. *J. Geophys. Res.* **2000**, *105*, 29039–29051. [[CrossRef](#)]
111. Anastasio, C.; Galbavy, E.S.; Hutterli, M.A.; Burkhardt, J.F.; Friel, D.K. Photoformation of hydroxyl radical on snow grains at Summit, Greenland. *Atmos. Environ.* **2007**, *41*, 5110–5121. [[CrossRef](#)]
112. Noro, K.; Hattori, S.; Uemura, R.; Fukui, K.; Hirabayashi, M.; Kawamura, K.; Motoyama, H.; Takenaka, N.; Yoshida, N. Spatial variation of isotopic compositions of snowpack nitrate related to post-depositional processes in eastern Dronning Maud Land, East Antarctica. *Geochem. J.* **2018**, *52*, e7–e14. [[CrossRef](#)]

Disclaimer/Publisher’s Note: The statements, opinions and data contained in all publications are solely those of the individual author(s) and contributor(s) and not of MDPI and/or the editor(s). MDPI and/or the editor(s) disclaim responsibility for any injury to people or property resulting from any ideas, methods, instructions or products referred to in the content.